

Feb. 2017

Probing the MSSM explanation of the muon g-2 anomaly in dark matter experiments and at a 100 TeV pp collider

Archil Kobakhidze¹, Matthew Talia¹ and Lei Wu^{1,2}

¹ *ARC Centre of Excellence for Particle Physics at the Terascale,
School of Physics, The University of Sydney, NSW 2006, Australia*

² *Department of Physics and Institute of Theoretical Physics, Nanjing Normal University,
Nanjing, Jiangsu 210023, China*

E-mails: archil.kobakhidze, matthew.talia, lei.wu1@sydney.edu.au

Abstract

We explore the ability of current and future dark matter and collider experiments in probing anomalous magnetic moment of the muon, $(g-2)_\mu$, within the Minimal Supersymmetric Standard Model (MSSM). We find that the latest PandaX-II/LUX-2016 data gives a strong constraint on parameter space that accommodates the $(g-2)_\mu$ within 2σ range, which will be further excluded by the upcoming XENON-1T (2017) experiment. We also find that a 100 TeV pp collider can cover most of our surviving samples that satisfy DM relic density within 3σ range through Z or h resonant effect by searching for trilepton events from $\tilde{\chi}_2^0 \tilde{\chi}_1^+$ associated production. While the samples that are beyond future sensitivity of trilepton search at a 100 TeV pp collider and the DM direct detections are either higgsino/wino-like LSPs or bino-like LSPs co-annihilating with sleptons. Such compressed regions may be covered by the monojet(-like) searches at a 100 TeV pp collider.

1 Introduction

The discovery of Higgs boson [1, 2] and subsequent measurements of its properties completed the Standard Model (SM) and provided it with very convincing evidence for the simplest perturbative realisation of the electroweak symmetry breaking (EWSB). Despite this overwhelming empirical success, our understanding of EWSB is incomplete. Namely, the quantum corrections are known to drive the Higgs mass (and hence the electroweak scale) towards high-energy scales and thus the SM requires unnaturally precise fine-tuning of parameters to satisfy the observations. In addition, observations of neutrino oscillations and dark matter (DM) certainly require beyond the standard model (BSM) physics.

Another deviation from the SM prediction are long seen in the measurements of the anomalous magnetic moment of the muon, $a_\mu = (g - 2)_\mu/2$ [3–6]. The recently measured value [7],

$$\Delta a_\mu^{\text{Exp-SM}} = \begin{cases} (28.7 \pm 8.0) \times 10^{-10} & [8], \\ (26.1 \pm 8.0) \times 10^{-10} & [9], \end{cases} \quad (1)$$

are more than 3σ away from the SM prediction, which includes improved QED [10] and electroweak [11] contributions. The upcoming experiments at NBL will measure the $(g - 2)_\mu$ with a precision of 0.14 ppm [12], which would potentially allow a 5σ discovery of new physics through such measurements. Needless to say, there are several candidate explanations for $(g - 2)_\mu$ anomaly proposed within various new physics frameworks.

The weak-scale supersymmetry (SUSY) has long been the dominant paradigm for new particle physics. The minimal supersymmetric standard model (MSSM) not only provides an elegant solution to the hierarchy problem but also may successfully explain $(g - 2)_\mu$ anomaly [13–33]. In the MSSM, the most significant contribution to a_μ is due to the one-loop diagrams involving the smuon $\tilde{\mu}$, muon sneutrino $\tilde{\nu}_\mu$, neutralinos $\tilde{\chi}^0$ and charginos $\tilde{\chi}^\pm$. The one-loop contribution to a_μ arises if there is a chirality flip between incoming and outgoing external muon lines, which may be induced through the $L - R$ mixing in the smuon sector or the SUSY Yukawa couplings of Higgsinos to muon and $\tilde{\mu}$ or $\tilde{\nu}_\mu$. Therefore, these contributions to a_μ are typically proportional to $m_\mu^2/M_{\text{SUSY}}^2$. Thus, to generate the sizable contributions to a_μ , the SUSY scale M_{SUSY} encapsulating slepton and electroweakino masses has to be around $O(100)$ GeV. So, the detection of light sleptons and electroweakinos will provide a test for the MSSM solution to the $(g - 2)_\mu$ problem.

The negative results of direct searches for sparticles during the LHC Run-1 have pushed up the mass limits of the first two generation squarks and gluino into the TeV region [34, 35]. The third generation squarks have been tightly constrained in the simplified models [36, 37], such as in Stealth SUSY [38] and Natural SUSY [39–44]. Unlike the colored sparticles, the bounds on the sleptons [45, 46] and electroweakinos [47, 48] are relatively weak, especially for the region of compressed spectrum. The lightest neutralino still remains as a successful dark matter (DM) candidate and significant

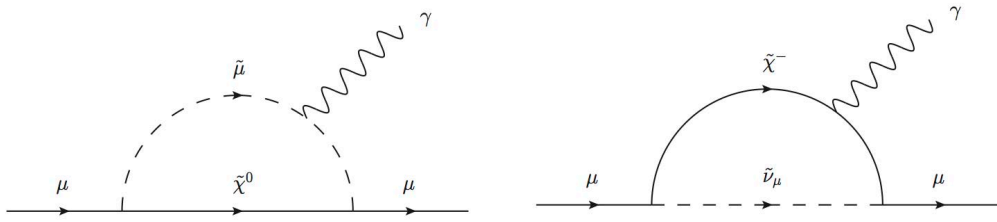


Figure 1: One-loop diagram contributions of the MSSM to the muon anomalous magnetic moment, $(g - 2)_\mu$. The first involves a smuon-neutralino (left) and the second a chargino-muon sneutrino loop (right).

effort has been made to obtain a lower mass limit on the neutralino LSP in MSSM, see e.g. [49–52].

In this paper, we explore the potential of the current and future dark matter and collider experiments to probe the anomalous magnetic moment of the muon within the MSSM. Using LEP and Higgs data and demanding that the theory accommodates $(g-2)_\mu$ measurements within 2σ range, we derive bounds on the electroweakino masses. Following this, we impose dark matter constraints from Planck, PandaX-II/LUX 2016 data and constraints from LHC searches for dilepton and trilepton events. Then, we evaluate the prospect of a future 100 TeV hadron collider in probing electroweakinos in trilepton events within this scenario. Finally, our conclusions are presented.

2 $(g - 2)_\mu$ in MSSM

The low-energy effective operator for magnetic dipole moment (MDM) is given by:

$$\mathcal{L}_{MDM} = \frac{e}{4m_\mu} a_\mu \bar{\mu} \sigma_{\rho\lambda} \mu F^{\rho\lambda}. \quad (2)$$

where e is the electric charge and m_μ is the muon mass. $F^{\rho\lambda}$ is the field strength of the photon field and $\sigma_{\rho\lambda} = \frac{i}{2}[\gamma_\rho, \gamma_\lambda]$.

In the MSSM, there are essentially two types of diagrams which contribute to a_μ at one-loop, i.e. one is the $\tilde{\chi}^0 - \tilde{\mu}$ loop diagram (left panel of Fig. 1) and the other is the chargino $\tilde{\chi}^\pm - \tilde{\nu}_\mu$ loop diagram (right panel of Fig. 1). The expressions for one-loop SUSY corrections to a_μ (including the complex phases effects) are given by [14]

$$a_\mu^{\tilde{\chi}^0} = \frac{m_\mu}{16\pi^2} \sum_{i,\alpha} \left\{ -\frac{m_\mu}{12m_{\tilde{\mu}_m}^2} (|n_{i\alpha}^L|^2 + |n_{i\alpha}^R|^2) F_1^N(x_{i\alpha}) + \frac{m_{\tilde{\chi}_i^0}}{3m_{\tilde{\mu}_m}^2} \text{Re}(n_{i\alpha}^L n_{i\alpha}^R) F_2^N(x_{i\alpha}) \right\} \quad (3)$$

$$a_\mu^{\tilde{\chi}^\pm} = \frac{m_\mu}{16\pi^2} \sum_j \left\{ \frac{m_\mu}{12m_{\tilde{\nu}_\mu}^2} (|c_j^L|^2 + |c_j^R|^2) F_1^C(x_j) + \frac{2m_{\tilde{\chi}_j^\pm}}{3m_{\tilde{\nu}_\mu}^2} \text{Re}(c_j^L c_j^R) F_2^C(x_j) \right\} \quad (4)$$

where $i = 1, 2, 3, 4$, $j = 1, 2$ and $\alpha = 1, 2$ denotes the neutralino, chargino and smuon mass eigenstates, respectively. The couplings are defined as

$$\begin{aligned} n_{i\alpha}^R &= \sqrt{2}g_1N_{i1}X_{\alpha 2} + y_\mu N_{i3}X_{\alpha 1}, \\ n_{i\alpha}^L &= \frac{1}{\sqrt{2}}(g_2N_{i2} + g_1N_{i1})X_{\alpha 1}^* - y_\mu N_{i3}X_{\alpha 2}^*, \\ c_j^R &= y_\mu U_{j2}, \\ c_j^L &= -g_2V_{j1}, \end{aligned} \quad (5)$$

where the muon Yukawa coupling $y_\mu = g_2m_\mu/\sqrt{2}m_W \cos \beta$. N are the neutralino and U, V are the chargino mixing matrices, respectively. X denotes the slepton mixing matrix. In terms of the kinematic variables $x_{i\alpha} = m_{\tilde{\chi}_i^0}/m_{\tilde{\mu}_\alpha}^2$ and $x_j = m_{\tilde{\chi}_j^\pm}/m_{\tilde{\nu}_\mu}^2$, the loop functions F are defined as follows

$$\begin{aligned} F_1^N(x) &= \frac{2}{(1-x)^4} \left[1 - 6x + 3x^2 + 2x^3 - 6x^2 \ln x \right], \\ F_2^N(x) &= \frac{3}{(1-x)^3} \left[1 - x^2 + 2x \ln x \right], \\ F_1^C(x) &= \frac{2}{(1-x)^4} \left[2 + 3x - 6x^2 + x^3 + 6x \ln x \right], \\ F_2^C(x) &= -\frac{3}{2(1-x)^3} \left[3 - 4x + x^2 + 2 \ln x \right]. \end{aligned} \quad (6)$$

These one-loop corrections mainly rely on the bino/wino masses $M_{1,2}$, the Higgsino mass μ , the left- and right-smuon mass parameters, $M_{\tilde{\mu}_L, \tilde{\mu}_R}$, and the ratio of the two Higgs vacuum expectation values, $\tan \beta$. They have a weak dependence on the second generation trilinear coupling A_μ . In the limit of large $\tan \beta$, when all the mass scales are roughly of the same order of M_{SUSY} , the contributions Eq. (3) and Eq. (4) can be approximately written as

$$a_\mu^{\tilde{\chi}^\pm} \simeq \frac{m_\mu^2 g_2^2}{32\pi^2 M_{SUSY}^2} \tan \beta; \quad (7)$$

$$a_\mu^{\tilde{\chi}^0} \simeq \frac{m_\mu^2}{192\pi^2 M_{SUSY}^2} (g_1^2 - g_2^2) \tan \beta. \quad (8)$$

The detailed dependence of a_μ on the five relevant mass parameters $\tan \beta$ is complicated. For two-loop corrections, it should be noted that if the squark masses (or masses of the first or third generation slepton) become large, the SUSY contributions to a_μ do not decouple but are logarithmically enhanced. Depending on the mass pattern, a positive or negative correction of $O(10\%)$ for squark masses in the few TeV region can be obtained, see Ref. [53].

3 Constraints on MSSM Explanation of $(g - 2)_\mu$

In the following, we numerically calculate Δa_μ by using the `FeynHiggs-2.12.0` [54] package and scan the relevant MSSM parameter space:

$$\begin{aligned} 10 < \tan \beta < 50, \quad -2 \text{ TeV} < M_1, M_2 < 2 \text{ TeV}, \\ -2 \text{ TeV} < \mu < 2 \text{ TeV}, \quad 0.1 \text{ TeV} < m_{\tilde{l}_L}, m_{\tilde{l}_R} < 2 \text{ TeV}. \end{aligned} \quad (9)$$

where we have the subscript $\ell = e, \mu$. Due to the small effects on a_μ , the slepton trilinear parameters of the first two generation are assumed as $A_\ell = 0$. We also decouple the stau sector by setting the soft stau mass parameters $m_{\tilde{\tau}_L} = m_{\tilde{\tau}_R} = 5$ TeV and trilinear parameter $A_\tau = 0$. So the stau will not contribute to the trilepton signals in our simulations. To satisfy the 125 GeV Higgs mass within a 2 GeV deviation, we vary the stop trilinear parameter in the range $|A_t| < 5$ TeV and set the stop soft masses at 5 TeV. We require the mixing parameter $|X_t/M_S| < 2$ to avoid the charge/colour-breaking minima [55]. We additionally calculate the Higgs mass and the rest of the sparticle masses with `FeynHiggs-2.12.0` [54].

3.1 LEP and Higgs data

In our scan, we also consider the following experimental bounds:

- LEP: the direct searches for the slepton and chargino at LEP produce the lower mass limits on the first two generation sleptons and lightest chargino [56]:

$$m_{\tilde{l}_L}, m_{\tilde{l}_R} > 100 \text{ GeV} \quad (l = e, \mu) \quad (10)$$

$$m_{\tilde{\chi}_1^\pm} > 105 \text{ GeV} \quad (11)$$

- Higgs data: the exclusion limits at 95% CL from the experimental cross sections from higgs searches at LEP, Tevatron and LHC are examined by using `HiggsBounds-4.2.1` [57].
- We require the lightest neutralino $\tilde{\chi}_1^0$ as the LSP and $m_{\tilde{\chi}_1^0} > 30$ GeV to be consistent with the bound on light MSSM neutralino dark matter [58].

In Fig. 2, we present the dependence of Δa_μ on the masses of neutralinos ($\tilde{\chi}_{1,2}^0$), charginos ($\tilde{\chi}_{1,2}^\pm$) and smuons ($\tilde{\mu}_{1,2}$). Within the scan ranges of Eq. 9, We find that the $\tilde{\chi}^\pm$ - $\tilde{\nu}_\mu$ loop dominates over the $\tilde{\chi}^0$ - $\tilde{\mu}$ loop. A sizable SUSY contribution to a_μ can be obtained, if M_1, M_2 and μ have the same sign and $\tilde{\chi}_{1,2}^0$ and $\tilde{\chi}_1^\pm$ have a sizable higgsino, wino or both components with large $\tan \beta$. The explanation of Δa_μ within a 2σ range requires $m_{\tilde{\chi}_1^0} < 1.0$ TeV and $m_{\tilde{\mu}_1} < 1.03$ TeV¹. However, a higgsino or wino-like LSP typically cannot satisfy the constraints of the dark matter relic density and are constrained using data from direct detection experiments.

¹It should be noted that if the higgsino mass parameter μ is large enough, the $g - 2$ anomaly may be explained through the bino-smuon loop contribution, due to the large smuon left-right mixing [59]. But such a large μ scenario is disfavored by the vacuum stability [59], the naturalness [60] and are highly constrained by the dark matter relic density [61].

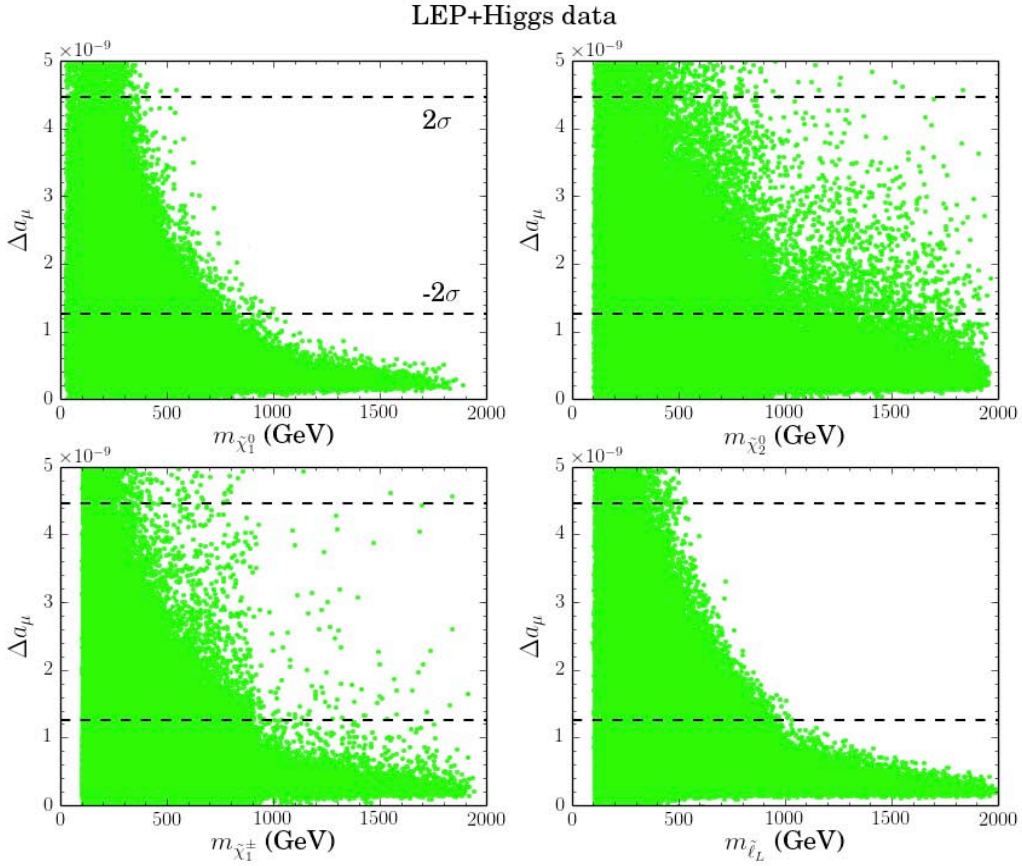


Figure 2: Scatter plot on the plane of Δa_μ and sparticle masses. Green circles satisfy the constraints from LEP and LHC Higgs data. The dashed lines represent the 2σ band on Δa_μ given by Eq.(1).

3.2 DM relic density and direct detection experiments

Next, we confront the MSSM explanation of $(g - 2)_\mu$ with the various dark matter experiments. We use `Micr0megas-4.2.3` [62] to calculate the dark matter relic density Ωh^2 and the spin-independent neutralino scattering cross sections with nuclei, denoted as σ^{SI} . It should be noted that the thermal relic abundance of the light higgsino or wino-like neutralino dark matter is typically low due to the large annihilation rate in the early universe. This leads to the standard thermally produced WIMP dark matter being under-abundant. In order to have the correct relic density, several alternatives have been proposed, such as choosing the axion-higgsino admixture as a dark matter candidate [63]. So we rescale the scattering cross section σ^{SI} by a factor of $(\Omega h^2 / \Omega_{Planck} h^2)$, where $\Omega_{Planck} h^2 = 0.112 \pm 0.006$ is the relic density measured by Planck satellite [64].

In Fig. 3, we show the neutralino dark matter relic density Ωh^2 (left) and the spin-

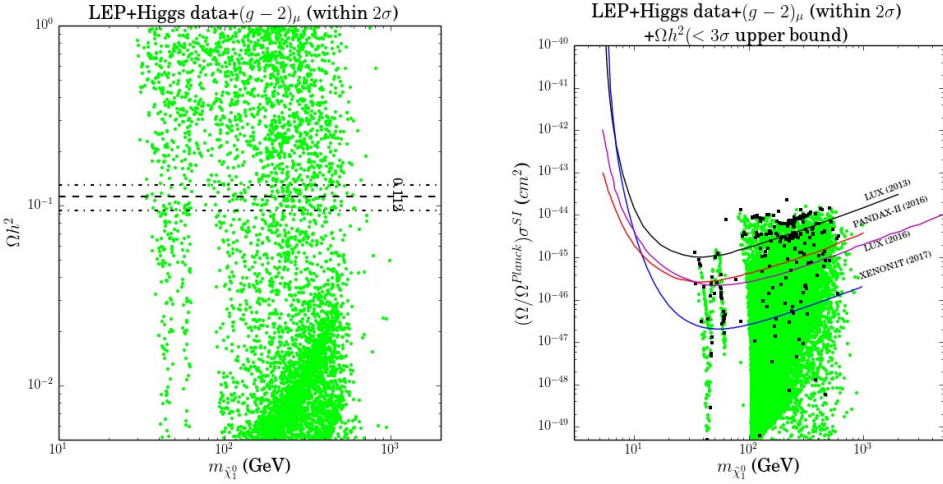


Figure 3: The neutralino dark matter relic density Ωh^2 (left) and the spin-independent neutralino-nucleon scattering cross section σ^{SI} (right). The dashed line is the PLANCK central value and the dashed-dotted lines are corresponding 3σ bands. The exclusion limits on the σ^{SI} from LUX (2013) [65] (black line), LUX (2016) (magenta line) [67], PandaX-II (red line) [66], and XENON1T (2017) projected [70] (blue line). Green circles satisfy the LEP, Higgs data and 2σ bound of $(g-2)_\mu$ (left) and 3σ upper bound of Ωh^2 , while the black squares further require Ωh^2 within 3σ range.

independent neutralino-nucleon scattering cross section σ^{SI} (right). All samples satisfy the LEP, Higgs data and $(g-2)_\mu$ within 2σ . In the left panel of Fig. 3, it can be seen that there are an amount of samples above the 3σ upper bound of the Planck relic density measurement. Those samples are bino-like and annihilate to the SM particles very slowly, which leads to an overabundance of dark matter in the universe. On the other hand, there are two dips around M_Z and M_h , respectively, where $\tilde{\chi}_1^0 \tilde{\chi}_1^0$ can efficiently annihilate through the resonance effect. When the LSP higgsino or wino component dominates, the annihilation cross section of $\tilde{\chi}_1^0 \tilde{\chi}_1^0$ is small so that the relic density is less than the 3σ lower bound of the Planck value. A mixed LSP with a certain higgsino or wino fraction [61] can be reconciled with the measured relic abundance Ωh^2 within the 3σ range. In the right panel of Fig. 3, we project the samples that satisfy 3σ upper bound $\Omega_{Planck} h^2$ on the plane of σ^{SI} versus $m_{\tilde{\chi}_1^0}$.

A significant portion of the parameter space where the LSP has a sizable higgsino or wino component is excluded by the recent PandaX-II [66] and LUX data [67]. The samples with nearly pure higgsino or wino LSPs escape experimental constraints due to the large reduction in the DM abundance. We also find some samples with the correct DM relic density (within 3σ) and satisfying the LUX constraints. These samples can be placed in two categories. The smaller portion of samples belong to the so called MSSM blind-spot region of parameters [68, 69] where the LSP coupling to the Higgs/Z boson is so small that the DM-nucleon scattering cross section is highly suppressed. The sfermions and other heavy higgs bosons are decoupled for these particular samples. The

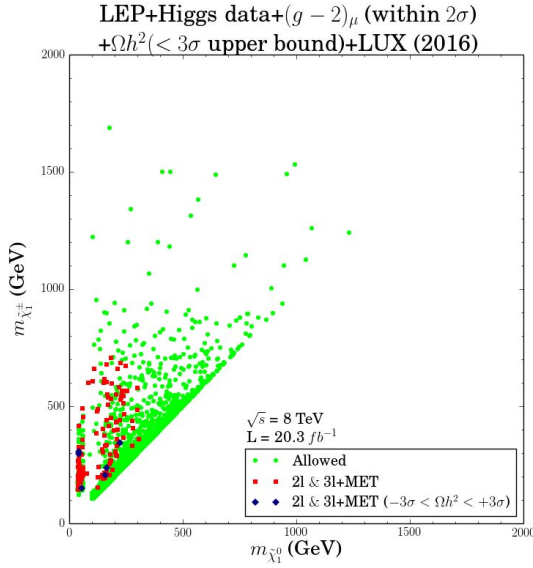


Figure 4: Exclusion limits from LHC Run-1 dilepton and trilepton events. All samples satisfy the LEP, Higgs data, 3σ upper bound of the dark matter relic density, LUX 2016 and $(g - 2)_\mu$ within the 2σ . Red squares ($\Omega h^2 < +3\sigma$) and blue diamonds ($-3\sigma < \Omega h^2 < +3\sigma$) are excluded by $2\ell + \cancel{E}_T$ and $3\ell + \cancel{E}_T$ events.

second case is that the bino-like LSPs coannihilate with the sleptons. The scattering cross section of the bino-like LSP with the nucleon can be small to avoid the LUX bound. The future XENON1T (2017) experiment [70] will further cover the these parameter space.

3.3 LHC 8 TeV collider search

Given the great progress of LHC experiments, we recast the results of searching for $2\ell + \cancel{E}_T$ and $3\ell + \cancel{E}_T$ signatures at LHC-8 TeV. We focus on 8 TeV data. In fact, most of dedicated analyses at 13 TeV are either preliminary [77–79] or do not provide stronger constraints in general due to the still small luminosity [80]. The main processes contributing to $2\ell + \cancel{E}_T$ events can arise from the production of sleptons pair and charginos:

$$pp \rightarrow \tilde{\ell}^+ \tilde{\ell}^-, \tilde{\chi}_1^+ \tilde{\chi}_1^- \quad (12)$$

with the subsequent decays to leptons:

- slepton decay: $\tilde{\ell}^\pm \rightarrow \ell^\pm \tilde{\chi}_1^0$;
- chargino decays: (a) through sleptons: $\tilde{\chi}_1^\pm \rightarrow \tilde{\ell}^\pm (\rightarrow \ell^\pm \tilde{\chi}_1^0) \nu_\ell$, (b) through sneutrinos: $\tilde{\chi}_1^\pm \rightarrow \tilde{\nu}_\ell (\rightarrow \nu_\ell \tilde{\chi}_1^0) \ell^\pm$, (c) through W boson: $\tilde{\chi}_1^\pm \rightarrow W^\pm (\rightarrow \ell^\pm \nu_\ell) \tilde{\chi}_1^0$.

While $3\ell + \cancel{E}_T$ events mainly come from the associated production of chargino and neutralino:

$$pp \rightarrow \tilde{\chi}_i^0 \tilde{\chi}_j^\pm \quad (13)$$

where $i = 2, 3, 4$ and $j = 1, 2$. They then decay in two different ways:

- through sleptons/sneutrinos: (a) $\tilde{\chi}_i^0 \rightarrow \ell^\mp \tilde{\ell}^\pm (\rightarrow \ell^\pm \tilde{\chi}_1^0)$, $\tilde{\chi}_j^\pm \rightarrow \tilde{\ell}^\pm (\rightarrow \ell^\pm \tilde{\chi}_1^0) \nu_\ell$, (b) $\tilde{\chi}_i^0 \rightarrow \ell^\mp \tilde{\ell}^\pm (\rightarrow \ell^\pm \tilde{\chi}_1^0)$, $\tilde{\chi}_j^\pm \rightarrow \tilde{\nu}_\ell (\rightarrow \nu_\ell \tilde{\chi}_1^0) \ell^\pm$;
- through the SM gauge bosons: $\tilde{\chi}_i^0 \rightarrow Z^{(*)} (\rightarrow \ell^\pm \ell^\mp) \tilde{\chi}_1^0$, $\tilde{\chi}_j^\pm \rightarrow W^{\pm(*)} (\rightarrow \ell^\pm \nu_\ell) \tilde{\chi}_1^0$.

We use **SPheno-3.3.8** [71] to produce the SLHA file to employ in **MadGraph5_aMC@NLO** [72] and generate the parton level signal events. Then the events are showered and hadronized by **PYTHIA** [73]. The detector effects are included by using the tuned **Delphes** [74]. **FastJet** [75] is used to cluster jets with the anti- k_t algorithm [76]. We recast the ATLAS dilepton [45] and trilepton [47] analyses by using **CheckMATE-1.2.2** [81]. We include the NLO correction effects in the production of $\tilde{\ell}^\pm \tilde{\ell}^\mp$, $\tilde{\chi}_i^\pm \tilde{\chi}_i^\mp$ and $\tilde{\chi}_i^0 \tilde{\chi}_j^\pm$ productions by multiplying a K -factor 1.3 [82]. The main SM backgrounds include WZ , ZZ and $t\bar{t}V(V = W, Z)$. To estimate the exclusion limit, we define the ratio $r = \max(N_{S,i}/S_{obs,i}^{95\%})$, where $N_{S,i}$ and $S_{obs,i}^{95\%}$ are the event numbers of the signal for i -th signal region and the corresponding observed 95% C.L. upper limit, respectively. The max is over all signal regions defined in the analysis. We conclude that a sample is excluded at 95% C.L., if $r > 1$.

In Fig. 4, we recast the LHC Run-1 dilepton and trilepton exclusion limits on the plane of $m_{\tilde{\chi}_1^\pm}$ and $m_{\tilde{\chi}_1^0}$. All samples satisfy the LEP, Higgs data, 3σ upper bound of relic density, LUX 2016 and $(g-2)_\mu$ within 2σ range. Red squares ($\Omega h^2 < +3\sigma$) and blue diamonds ($-3\sigma < \Omega h^2 < +3\sigma$) are excluded by $2\ell + \cancel{E}_T$ and $3\ell + \cancel{E}_T$ events. In Fig. 4, we can see that a portion of samples in $\tilde{\chi}_1^\pm < 710$ GeV and $\tilde{\chi}_1^0 < 300$ GeV can be excluded. A bulk of samples in the parameter space with $\tilde{\chi}_1^0$ being higgsino or wino-like can not be covered because of the small mass difference between $\tilde{\chi}_1^\pm$ and $\tilde{\chi}_1^0$. Such a region may be accessed by the monojet(-like) or the VBF production at HL-LHC [83–89]. In addition, when $\tilde{\chi}_2^0$ has a sizable bino component, the limit from trilepton events will become weak because of the reduction of cross section of $\tilde{\chi}_1^\pm \tilde{\chi}_2^0$. We also find that the dilepton channel can be complimentary to the trilepton channel when the latter is suppressed by small neutralino leptonic branching ratios. An important factor in the dilepton and trilepton yields is the leptonic branching fraction which can vary widely throughout the parameter space. If the slepton is on shell, the chargino two-body decays then dominate and its leptonic branching fraction is maximized, $Br(\tilde{\chi}_1^\pm \rightarrow \tilde{\chi}_1^0 \tilde{\ell}^\pm (\rightarrow \ell^\pm \nu_\ell))_{max} = 2/3$. When the sneutrino is on-shell and is lighter than the corresponding slepton, the channel $\tilde{\chi}_2^0 \rightarrow \nu_\ell \tilde{\nu}_\ell$ will dominate the decay width, and the neutralino leptonic branching ratio is suppressed. On the other hand, if the slepton and sneutrino are heavy enough, the decay amplitudes of $\tilde{\chi}_1^\pm$ and $\tilde{\chi}_2^0$ are dominated by W and Z boson exchange, respectively, which give $\tilde{\chi}_1^\pm \rightarrow \tilde{\chi}_1^0 W^\pm (\rightarrow \ell^\pm \nu_\ell) \simeq 2/9$ and $\tilde{\chi}_2^0 \rightarrow \tilde{\chi}_1^0 Z (\rightarrow \ell^\pm \ell^\mp) \simeq 6\%$. On the other hand, $\tilde{\chi}_2^0$ can decay to $h \tilde{\chi}_1^0$

with a sizable branching ratio if kinematically accessible, which can also weaken the trilepton exclusion limit.

4 Prospects at a 100 TeV Collider

To hunt for new fundamental particles, a 100 TeV pp collider has been under discussion in recent years, which will allow us to probe the new physics scale roughly an order of magnitude higher than we can possibly reach with the LHC [90]. In this section, we estimate the prospects of probing the MSSM explanation of the $(g - 2)_\mu$ anomaly by extrapolating the above 8 TeV trilepton analysis to a 100 TeV pp collider. For each allowed sample above, we use the most sensitive signal region in 8 TeV analysis and simply assume the same detection efficiency in the 100 TeV analysis. We rescale the signal (S) and background (B) events by the following ratio:

$$N^{100\text{ TeV}} = (\sigma^{100\text{ TeV}}/\sigma^{8\text{ TeV}})(3000\text{ fb}^{-1}/20.3\text{ fb}^{-1})N^{8\text{ TeV}} \quad (14)$$

Such a treatment can be considered as a preliminary theoretical estimation. The optimized analysis strategy may be achieved once the details of the collider environment is known. To obtain the expected exclusion limits, we use the following equation,

$$\frac{S}{\sqrt{B + (\beta_{sys}B)^2}} \geq 2 \quad [\text{Excluded}] \quad (15)$$

where the factor β_{sys} parameterizes the systematic uncertainty. In Fig. 4, we can see that when $\beta_{sys} = 0.1$, a majority of samples allowed by $(g - 2)_\mu$ in the parameter space with $\tilde{\chi}_1^0 < 530$ GeV and $\tilde{\chi}_1^\pm < 940$ GeV can be excluded. Such a range will be extended to $\tilde{\chi}_1^0 < 710$ GeV and $\tilde{\chi}_1^\pm < 940$ GeV, if $\beta_{sys} = 0$.

It should be noted that the region that satisfies the DM relic density within the 3σ range through the Z or h resonant annihilation in the blind spots can be covered by searching for trilepton events from $\tilde{\chi}_2^0\tilde{\chi}_1^+$ associated production at a 100 TeV pp collider. The samples that are beyond future sensitivity of this trilepton search and the DM direct detections are either higgsino/wino-like LSPs with the compressed mass spectrum or bino-like LSPs co-annihilating with sleptons. Such compressed regions may be probed by the monojet(-like) searches at a 100 TeV pp collider [91].

5 Conclusion

In this work we have studied the prospect of current and future dark matter and collider experiments in probing the anomalous magnetic moment of the muon in the MSSM. Under the constraints of Higgs data, dark matter relic density, PandaX-II/LUX-2016 experiments and LHC-8 TeV searches for dilepton/trilepton events, we find the Planck data and the recent PandaX-II/LUX data can significantly exclude the MSSM parameter space satisfying $(g - 2)_\mu$, which will be further excluded by the upcoming

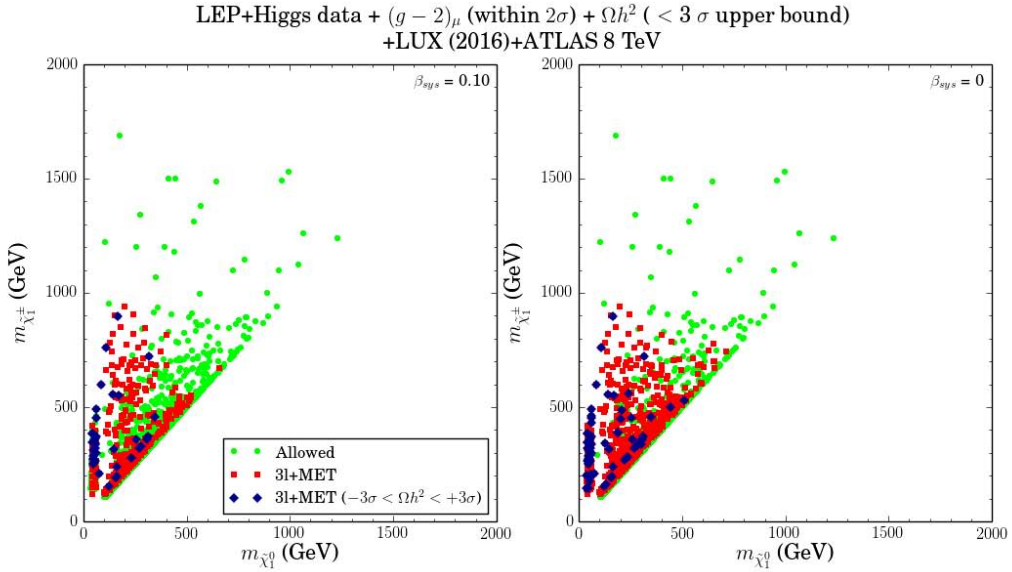


Figure 5: Same as Fig. 4, but for expected exclusion limit at a 100 TeV pp collider with the luminosity of 3000 fb^{-1} . Red squares ($\Omega h^2 < +3\sigma$) and blue diamonds $-3\sigma < \Omega h^2 < +3\sigma$ are excluded by searching for $3\ell + \text{MET}$ events. The systematic uncertainty β_{sys} is taken as 0.1 and 0, respectively.

XENON-1T (2017) experiment. We also find that most of our surviving samples that satisfy DM relic density within 3σ range through Z or h resonant effect can be covered by searching for trilepton events from $\tilde{\chi}_2^0 \tilde{\chi}_1^+$ associated production at a 100 TeV pp collider. While the samples that are beyond the future sensitivity of this trilepton search and DM direct detections are either higgsino/wino-like LSPs or bino-like LSPs co-annihilating with sleptons. Such compressed regions may be probed by the monojet(-like) searches at a future 100 TeV pp collider.

Acknowledgement. This work was partially supported by the Australian Research Council. LW was also supported in part by the National Natural Science Foundation of China (NNSFC) under grants Nos. 11305049, 11275057.

References

- [1] G. Aad *et al.* [ATLAS Collaboration], Phys. Lett. B **716**, 1 (2012).
- [2] S. Chatrchyan *et al.* [CMS Collaboration], Phys. Lett. B **716**, 30 (2012).
- [3] K. Hagiwara, A. D. Martin, D. Nomura and T. Teubner, Phys. Lett. B **557**, 69 (2003) doi:10.1016/S0370-2693(03)00138-2 [hep-ph/0209187].
- [4] F. Jegerlehner and A. Nyffeler, Phys. Rept. **477**, (2009) 1.

- [5] J. P. Miller, E. de Rafael, B. L. Roberts and D. Stöckinger, Ann. Rev. Nucl. Part. Sci. **62**, 237 (2012).
- [6] T. Blum, A. Denig, I. Logashenko, E. de Rafael, B. L. Roberts, T. Teubner and G. Venanzoni, arXiv:1311.2198 [hep-ph].
- [7] G. W. Bennett *et al.* [Muon g-2 Collaboration], Phys. Rev. D **73**, 072003 (2006).
- [8] M. Davier, A. Hoecker, B. Malaescu and Z. Zhang, Eur. Phys. J. C **71**, 1515 (2011) Erratum: [Eur. Phys. J. C **72**, 1874 (2012)].
- [9] K. Hagiwara, R. Liao, A. D. Martin, D. Nomura and T. Teubner, J. Phys. G **38**, 085003 (2011).
- [10] T. Aoyama, M. Hayakawa, T. Kinoshita and M. Nio, Phys. Rev. Lett. **109**, 111808 (2012).
- [11] C. Gnendiger, D. Stöckinger and H. Stöckinger-Kim, Phys. Rev. D **88**, 053005 (2013).
- [12] G. Venanzoni [Fermilab E989 Collaboration], Nucl. Part. Phys. Proc. **273-275**, 584 (2016).
- [13] T. Moroi, Phys. Rev. D **53**, 6565 (1996) Erratum: [Phys. Rev. D **56**, 4424 (1997)].
- [14] S. P. Martin and J. D. Wells, Phys. Rev. D **64**, 035003 (2001).
- [15] D. Stöckinger, J. Phys. G **34**, R45 (2007).
- [16] G. -C. Cho, K. Hagiwara, Y. Matsumoto and D. Nomura, JHEP **1111**, 068 (2011).
- [17] M. Endo, K. Hamaguchi, S. Iwamoto and T. Yoshinaga, JHEP **1401**, 123 (2014).
- [18] M. Ibe, T. T. Yanagida and N. Yokozaki, JHEP **1308**, 067 (2013).
- [19] S. Akula and P. Nath, Phys. Rev. D **87**, no. 11, 115022 (2013).
- [20] S. Mohanty, S. Rao and D. P. Roy, JHEP **1309**, 027 (2013).
- [21] K. Kowalska, L. Roszkowski, E. M. Sessolo and A. J. Williams, arXiv:1503.08219 [hep-ph].
- [22] F. Wang, W. Wang, J. M. Yang and Y. Zhang, JHEP **1507**, 138 (2015).
- [23] F. Wang, W. Wang and J. M. Yang, JHEP **1506**, 079 (2015).
- [24] F. Wang, L. Wu, J. M. Yang and M. Zhang, Phys. Lett. B **759**, 191 (2016).

- [25] N. Okada, S. Raza and Q. Shafi, Phys. Rev. D **90**, no. 1, 015020 (2014) [arXiv:1307.0461 [hep-ph]].
- [26] I. Gogoladze, F. Nasir, Q. Shafi and C. S. Un, Phys. Rev. D **90** (2014) 3, 035008.
- [27] K. S. Babu, I. Gogoladze, Q. Shafi and C. S. Ün, Phys. Rev. D **90**, no. 11, 116002 (2014).
- [28] M. A. Ajaib, I. Gogoladze, Q. Shafi and C. S. Ün, JHEP **1405**, 079 (2014).
- [29] M. A. Ajaib, B. Dutta, T. Ghosh, I. Gogoladze and Q. Shafi, Phys. Rev. D **92**, no. 7, 075033 (2015).
- [30] M. Adeel Ajaib, I. Gogoladze and Q. Shafi, Phys. Rev. D **91**, no. 9, 095005 (2015).
- [31] I. Gogoladze, Q. Shafi and C. S. Ün, Phys. Rev. D **92**, no. 11, 115014 (2015).
- [32] M. Badziak, Z. Lalak, M. Lewicki, M. Olechowski and S. Pokorski, JHEP **1503** (2015) 003.
- [33] P. Athron *et al.*, Eur. Phys. J. C **76**, no. 2, 62 (2016).
- [34] G. Aad *et al.* [ATLAS Collaboration], JHEP **1310**, 130 (2013) Erratum: [JHEP **1401**, 109 (2014)].
- [35] S. Chatrchyan *et al.* [CMS Collaboration], JHEP **1406**, 055 (2014).
- [36] G. Aad *et al.* [ATLAS Collaboration], JHEP **1411**, 118 (2014).
- [37] S. Chatrchyan *et al.* [CMS Collaboration], Eur. Phys. J. C **73**, no. 12, 2677 (2013).
- [38] J. Fan, R. Krall, D. Pinner, M. Reece and J. T. Ruderman, JHEP **1607**, 016 (2016).
- [39] C. Han, K. i. Hikasa, L. Wu, J. M. Yang and Y. Zhang, JHEP **1310**, 216 (2013).
- [40] A. Kobakhidze, N. Liu, L. Wu, J. M. Yang and M. Zhang, Phys. Lett. B **755**, 76 (2016).
- [41] M. Drees and J. S. Kim, Phys. Rev. D **93**, no. 9, 095005 (2016).
- [42] C. Han, K. i. Hikasa, L. Wu, J. M. Yang and Y. Zhang, arXiv:1612.02296 [hep-ph].
- [43] G. H. Duan, K. i. Hikasa, L. Wu, J. M. Yang and M. Zhang, arXiv:1611.05211 [hep-ph].

[44] C. Han, J. Ren, L. Wu, J. M. Yang and M. Zhang, Eur. Phys. J. C **77**, no. 2, 93 (2017) doi:10.1140/epjc/s10052-017-4662-7 [arXiv:1609.02361 [hep-ph]].

[45] The ATLAS collaboration [ATLAS Collaboration], ATLAS-CONF-2013-049.

[46] V. Khachatryan *et al.* [CMS Collaboration], Eur. Phys. J. C **74**, no. 9, 3036 (2014).

[47] G. Aad *et al.* [ATLAS Collaboration], JHEP **1404**, 169 (2014).

[48] V. Khachatryan *et al.* [CMS Collaboration], Phys. Rev. D **90**, no. 9, 092007 (2014).

[49] J. Ellis and K. A. Olive, Eur. Phys. J. C **72**, 2005 (2012).

[50] H. Baer, V. Barger and A. Mustafayev, JHEP **1205**, 091 (2012).

[51] G. Bélanger, G. Drieu La Rochelle, B. Dumont, R. M. Godbole, S. Kraml and S. Kulkarni, Phys. Lett. B **726**, 773 (2013).

[52] M. Cahill-Rowley, R. Cotta, A. Drlica-Wagner, S. Funk, J. Hewett, A. Ismail, T. Rizzo and M. Wood, Phys. Rev. D **91**, no. 5, 055011 (2015).

[53] H. Farnoli, C. Gnendiger, S. Paßehr, D. Stöckinger and H. Stöckinger-Kim, JHEP **1402**, 070 (2014).

[54] S. Heinemeyer, W. Hollik and G. Weiglein, Comput. Phys. Commun. **124**, 76 (2000); Eur. Phys. J. C **9**, 343 (1999).

[55] U. Chattopadhyay and A. Dey, JHEP **1411**, 161 (2014).

[56] K. A. Olive *et al.* [Particle Data Group Collaboration], Chin. Phys. C **38**, 090001 (2014).

[57] P. Bechtle *et al.*, Comput. Phys. Commun. **182**, 2605 (2011); Comput. Phys. Commun. **181**, 138 (2010).

[58] L. Calibbi, J. M. Lindert, T. Ota and Y. Takanishi, JHEP **1411**, 106 (2014).

[59] M. Endo, K. Hamaguchi, T. Kitahara and T. Yoshinaga, JHEP **1311**, 013 (2013) doi:10.1007/JHEP11(2013)013 [arXiv:1309.3065 [hep-ph]].

[60] R. Arnowitt and P. Nath, Phys. Rev. D **46**, 3981 (1992).

[61] N. Arkani-Hamed, A. Delgado and G. F. Giudice, Nucl. Phys. B **741**, 108 (2006) doi:10.1016/j.nuclphysb.2006.02.010 [hep-ph/0601041].

[62] G. Belanger *et al.*, Comput. Phys. Commun. **182**, 842 (2011).

- [63] H. Baer, A. Lessa, S. Rajagopalan and W. Sreethawong, JCAP **1106** (2011) 031.
- [64] P. A. R. Ade *et al.* [Planck Collaboration], arXiv:1502.01589 [astro-ph.CO].
- [65] D. S. Akerib *et al.* [LUX Collaboration], Phys. Rev. Lett. **112** (2014) 091303.
- [66] A. Tan *et al.* [PandaX-II Collaboration], Phys. Rev. Lett. **117**, no. 12, 121303 (2016) doi:10.1103/PhysRevLett.117.121303 [arXiv:1607.07400 [hep-ex]].
- [67] D. S. Akerib *et al.*, arXiv:1608.07648 [astro-ph.CO].
- [68] C. Cheung, L. J. Hall, D. Pinner and J. T. Ruderman, JHEP **1305**, 100 (2013) doi:10.1007/JHEP05(2013)100 [arXiv:1211.4873 [hep-ph]].
- [69] T. Han, F. Kling, S. Su and Y. Wu, [arXiv:1612.02387 [hep-ph]].
- [70] XENON1T Collaboration, E. Aprile, *et al.*, arXiv:1206.6288.
- [71] W. Porod, Comput. Phys. Commun. **153**, 275 (2003) doi:10.1016/S0010-4655(03)00222-4 [hep-ph/0301101].
- [72] J. Alwall *et al.*, JHEP **1407**, 079 (2014).
- [73] T. Sjostrand, S. Mrenna and P. Z. Skands, JHEP **0605**, 026 (2006).
- [74] J. de Favereau, *et al.*, arXiv:1307.6346 [hep-ex].
- [75] M. Cacciari, G. P. Salam and G. Soyez, Eur. Phys. J. C **72**, 1896 (2012) [arXiv:1111.6097 [hep-ph]].
- [76] M. Cacciari, G. P. Salam and G. Soyez, JHEP **0804**, 063 (2008).
- [77] ATLAS-CONF-2016-075
- [78] CMS-PAS-SUS-16-024.
- [79] CMS-PAS-SUS-16-022
- [80] G. Aad *et al.* [ATLAS Collaboration], Eur. Phys. J. C **76**, no. 5, 259 (2016) doi:10.1140/epjc/s10052-016-4095-8 [arXiv:1602.09058 [hep-ex]].
- [81] M. Drees *et al.*, Comput. Phys. Commun. **187**, 227 (2014).
- [82] W. Beenakker, R. Hopker and M. Spira, hep-ph/9611232.
- [83] A. Barr and J. Scoville, JHEP **1504**, 147 (2015).
- [84] P. Schwaller and J. Zurita, JHEP **1403**, 060 (2014).

- [85] C. Han, A. Kobakhidze, N. Liu, A. Saavedra, L. Wu and J. M. Yang, JHEP **1402**, 049 (2014).
- [86] H. Baer, A. Mustafayev and X. Tata, Phys. Rev. D **89**, no. 5, 055007 (2014).
- [87] C. Han, L. Wu, J. M. Yang, M. Zhang and Y. Zhang, Phys. Rev. D **91**, 055030 (2015).
- [88] B. Dutta *et al.*, Phys. Rev. D **91**, no. 5, 055025 (2015).
- [89] B. Dutta *et al.*, Phys. Rev. D **90**, no. 9, 095022 (2014).
- [90] N. Arkani-Hamed, T. Han, M. Mangano and L. T. Wang, arXiv:1511.06495 [hep-ph].
- [91] M. Low and L. T. Wang, JHEP **1408**, 161 (2014).